PERGAMON

International Journal of Solids and Structures 40 (2003) 6577–6592

INTERNATIONAL JOURNAL OF SOLIDS and STRUCTURES

www.elsevier.com/locate/ijsolstr

Analysis of stress intensity factors of a ring-shaped interface crack

Nao-Aki Noda [a,*], Masayuki Kagita [a], Meng-Cheng Chen [a], Kazuhiro Oda [b]

[a] *Department of Mechanical Engineering, Kyushu Institute of Technology, 1-1 Sensuicho, Tobata, Kitakyushu 804-8550, Japan*

[b] *Department of Mechanical and Electrical Engineering, Tokuyama College of Technology, Tokuyama 745-8585, Japan*

Received 25 April 2003; received in revised form 25 April 2003

Abstract

In this paper, numerical solutions of singular integral equations are discussed in the analysis of axi-symmetric interface cracks under torsion and tension. The problems of a ring-shaped interface crack are formulated in terms of a system of singular integral equations on the basis of the body force method. In the numerical analysis, unknown body force densities are approximated by the products of the fundamental density functions and power series, where the fundamental densities are chosen to express a two-dimensional interface crack exactly. The accuracy of the present analysis is verified by comparing the present results with the results obtained by other researchers for the limiting cases of the geometries. The calculation shows that the present method gives rapidly converging numerical results for those problems as well as for ordinary crack problems in homogeneous material. The stress intensity factors of a ring-shaped interface crack are shown in tables and charts with varying the material combinations and also geometrical conditions.

Keywords: Elasticity; Interface crack; Stress intensity factor; Body force method; Singular integral equation

1. Introduction

In recent years the use of composite materials has been increasing in a wide area and accurate evaluation of interface strength in dissimilar materials has become very important. Considerable research has been done to evaluate the stress intensity factors (Salganik, 1963; Erdogan, 1963; England, 1965; Rice and Sih, 1965; Willis, 1971; Comninou, 1977; Tucker, 1974; Erdogan and Gupta, 1975; Zhang, 1984; Delale, 1985; Noda and Oda, 1997). However, most of these works are on two-dimensional cases except for some studies (Mossakovski and Rybka, 1964; Erdogan, 1965; Kassir and Bregman, 1972; Willis, 1972; Lowengrub and Sneddon, 1974; Keer et al., 1978; Sibuya et al., 1989; Yuuki and Cho, 1989). It should be noted that most studies for three-dimensional interface cracks are limited to the calculation for specific dimensions under special combination of the materials. In other words, closed form solutions are available only for a circular

* Corresponding author. Tel./fax: +81-93-884-3124.
E-mail address: noda@mech.kyutech.ac.jp (N.-A. Noda).

0020-7683/$ - see front matter
doi:10.1016/S0020-7683(03)00245-2

interface crack (Kassir and Bregman, 1972), and a deep circumferential interface crack (Takakuda et al., 1978).

In the previous study (Chen et al., 1999), hypersingular intergro-differential equations for the planar interface crack were indicated. However, the oscillation singularity as well as overlapping of crack surfaces near the crack tip makes it much more difficult exactly to solve the equations compared with the cases of ordinary cracks. In this paper, therefore, numerical solutions are considered for axi-symmetric interface cracks on the basis of the equations. Then, it is shown that the proposed method gives stress intensity factors accurately from the values of crack opening displacement obtained from numerical solutions.

2. Singular integral equations of a ring-shaped interface crack

2.1. Singular integral equations of three-dimensional interface crack

Singular integral equations for three-dimensional crack problem on bimaterial interface in Fig. 1 were derived by Chen et al. (1999) as shown in Eq. (1).

$$\begin{aligned}
&\mu_1(\Lambda_2-\Lambda_1)\frac{\partial\Delta u_z(x,y)}{\partial x}+\mu_1\frac{(2\Lambda-\Lambda_1-\Lambda_2)}{2\pi}\int_S\frac{1}{r^3}\Delta u_x(\xi)\,\mathrm{d}S(\xi)\\
&\quad+3\mu_1\frac{(\Lambda_1+\Lambda_2-\Lambda)}{2\pi}\left\{\int_S\frac{(x-\xi)^2}{r^5}\Delta u_x(\xi)\,\mathrm{d}S(\xi)+\int_S\frac{(x-\xi)(y-\eta)}{r^5}\Delta u_y(\xi)\,\mathrm{d}S(\xi)\right\}\\
&\quad=-p_x(x,y),\quad x,y\in S
\end{aligned}\tag{1a}$$

$$\begin{aligned}
&\mu_1(\Lambda_2-\Lambda_1)\frac{\partial\Delta u_z(x,y)}{\partial y}+\mu_1\frac{(2\Lambda-\Lambda_1-\Lambda_2)}{2\pi}\int_S\frac{1}{r^3}\Delta u_y(\xi)\,\mathrm{d}S(\xi)\\
&\quad+3\mu_1\frac{(\Lambda_1+\Lambda_2-\Lambda)}{2\pi}\left\{\int_S\frac{(x-\xi)(y-\eta)}{r^5}\Delta u_x(\xi)\,\mathrm{d}S(\xi)+\int_S\frac{(y-\eta)^2}{r^5}\Delta u_y(\xi)\,\mathrm{d}S(\xi)\right\}\\
&\quad=-p_y(x,y),\quad x,y\in S
\end{aligned}\tag{1b}$$

$$\mu_1(\Lambda_1-\Lambda_2)\left\{\frac{\partial\Delta u_x(x,y)}{\partial x}+\frac{\partial\Delta u_y(x,y)}{\partial y}\right\}+\mu_1\frac{(\Lambda_1+\Lambda_2)}{2\pi}\int_S\frac{1}{r^3}\Delta u_z(\xi)\,\mathrm{d}S(\xi)=-p_z(x,y),\quad x,y\in S\tag{1c}$$

$$\begin{aligned}
&\Lambda=\mu_2/(\mu_1+\mu_2),\quad \Lambda_1=\mu_2/(\mu_1+\kappa_1\mu_2),\quad \Lambda_2=\mu_2/(\mu_2+\kappa_2\mu_1),\quad \kappa_1=3-4\nu_1,\\
&\kappa_2=3-4\nu_2,\quad r^2=(x-\xi)^2+(y-\eta)^2
\end{aligned}\tag{1d}$$

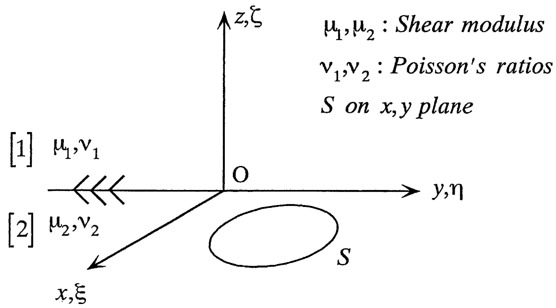

Fig. 1. Three-dimensional interface crack.

$$\Delta u_i(x,y) = u_i(x,y,0^+) - u_i(x,y,0^-) \quad (i = x,y,z) \tag{1e}$$

In Eq. (1), unknown functions are crack opening displacements, in other words, displacement discontinuities Δu_x, Δu_y, Δu_z defined in Eq. (1e). Here, (x,y,z) is a point of question, and (ξ,η,ζ) is a point where the displacement discontinuities are applied. The notations p_x, p_y, p_z are stresses τ_{yz}, τ_{zx}, σ_z at infinity, respectively, and ν_1, ν_2 are Poisson's ratios. Here, the integration should be interpreted in the sense of a finite part integral.

2.2. Singular integral equation for an axi-symmetric interface crack under torsion

In this paper, a ring-shaped interface crack as shown in Fig. 2 is considered. First, singular integral equation of a ring-shaped interface crack subjected to uniform torsion will be derived. By substituting $\Delta u_x = -\Delta u_\theta \sin\varphi$, $\Delta u_y = \Delta u_\theta \cos\varphi$, $\Delta u_z = 0$, $x = r$, $y = 0$, $\xi = \rho\cos\varphi$, $\eta = \rho\sin\varphi$ into Eqs. (1a), (1b), (1c) and considering $\partial/\partial\theta = 0$, $p_x = p_z = 0$, Eqs. (1a), (1c) will vanish.

Then, Eq. (1b) becomes Eq. (2). Here, (r,θ,z) is a cylindrical coordinate in question, and $(\rho,\varphi,0)$ is a cylindrical coordinate where the displacement discontinuities are applied.

$$\begin{aligned}
&\mu_1 \frac{(2\Lambda - \Lambda_1 - \Lambda_2)}{2\pi} \int_{r_i}^{r_o} \Delta u_\theta \int_0^{2\pi} \frac{\cos\varphi}{r^3} \rho \,\mathrm{d}\varphi \,\mathrm{d}\rho \\
&\quad + 3\mu_1 \frac{(\Lambda_1 + \Lambda_2 - \Lambda)}{2\pi} \left[\int_{r_i}^{r_o} \Delta u_\theta \int_0^{2\pi} \frac{(r - \rho\cos\varphi)(-\rho\sin\varphi)(-\sin\varphi)}{r^5} \rho \,\mathrm{d}\varphi \,\mathrm{d}\rho \right. \\
&\quad \left. + \int_{r_i}^{r_o} \Delta u_\theta \int_0^{2\pi} \frac{(\rho\sin\varphi)^2 \cos\varphi}{r^5} \rho \,\mathrm{d}\varphi \,\mathrm{d}\rho \right] = -p_y
\end{aligned} \tag{2}$$

Eq. (2) is reduced to Eq. (3a). Here, $K(k)$, $E(k)$ are a complete elliptic integral of first and second.

$$\frac{1}{\pi} \frac{\mu_1\mu_2}{\mu_1 + \mu_2} \int_{r_i}^{r_o} \Delta u_\theta \left\{ \frac{r^2 + \rho^2}{(r+\rho)(r-\rho)^2 r} E - \frac{1}{(r+\rho) r} K \right\} \mathrm{d}\rho = -p_y \tag{3a}$$

$$\left. \begin{aligned}
&e = 1 + \frac{(r-\rho)^2}{2r\rho}, \quad k = \sqrt{\frac{2}{e+1}} \\
&K(k) = \int_0^{\pi/2} \frac{\mathrm{d}\lambda}{\sqrt{1 - k^2\sin^2\lambda}}, \quad E(k) = \int_0^{\pi/2} \sqrt{1 - k^2\sin^2\lambda}\,\mathrm{d}\lambda
\end{aligned} \right\} \tag{3b}$$

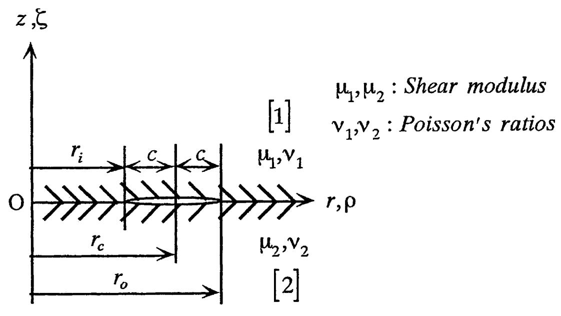

Fig. 2. Ring-shaped interface crack.

By substituting $r = r_c + r'$, $\rho = r_c + \rho'$ into Eq. (3a) and putting $r_c \to \infty$, we obtain the following equation:

$$\frac{1}{\pi}\frac{\mu_1\mu_2}{\mu_1+\mu_2}\int_{r_i}^{r_o}\Delta u_\theta\frac{1}{(r'-\rho')^2}\,\mathrm{d}\rho' = -p_y \tag{4}$$

This equation coincides with the equation of a two-dimensional interface crack subjected to anti-plane shear (for example, Erdogan and Gupta, 1975).

2.3. Singular integral equations for an axi-symmetric interface crack under tension

Next, singular integral equation of a ring-shaped interface crack subjected to uniform tension in the z-direction will be derived. By substituting $\Delta u_x = \Delta u_r\cos\varphi$, $\Delta u_y = \Delta u_r\sin\varphi$, $x = r$, $y = 0$, $\xi = \rho\cos\varphi$, $\eta = \rho\sin\varphi$ into Eqs. (1a), (1b), (1c) and considering $p_y = 0$, $\Delta u_y = 0$, $\partial/\partial y = 0$, Eq. (1b) will vanish. Then, we have

$$\begin{aligned}
&\mu_1(\Lambda_2-\Lambda_1)\frac{\partial\Delta u_z}{\partial r} + \mu_1\frac{(2\Lambda-\Lambda_1-\Lambda_2)}{2\pi}\int_{r_i}^{r_o}\Delta u_r\int_0^{2\pi}\frac{\cos\varphi}{r^3}\rho\,\mathrm{d}\varphi\,\mathrm{d}\rho\\
&\quad + 3\mu_1\frac{(\Lambda_1+\Lambda_2-\Lambda)}{2\pi}\left[\int_{r_i}^{r_o}\Delta u_r\int_0^{2\pi}\frac{(r-\rho\cos\varphi)^2\cos\varphi}{r^5}\rho\,\mathrm{d}\varphi\,\mathrm{d}\rho\right.\\
&\quad \left.+\int_{r_i}^{r_o}\Delta u_r\int_0^{2\pi}\frac{(r-\rho\cos\varphi)(-\rho\sin\varphi)\sin\varphi}{r^5}\rho\,\mathrm{d}\varphi\,\mathrm{d}\rho\right] = -p_x
\end{aligned} \tag{5a}$$

$$\mu_1(\Lambda_1-\Lambda_2)\frac{\partial\Delta u_r\cos\theta}{\partial r} + \mu_1\frac{(\Lambda_1+\Lambda_2)}{2\pi}\int_{r_i}^{r_o}\Delta u_z\int_0^{2\pi}\frac{1}{r^3}\rho\,\mathrm{d}\varphi\,\mathrm{d}\rho = -p_z \tag{5b}$$

Eqs. (5a), (5b) are reduced to Eqs. (6a), (6b), respectively.

$$-\beta C\frac{\partial\Delta u_r\cos\theta}{\partial r} + \frac{C}{\pi}\int_{r_i}^{r_o}\Delta u_z\frac{2}{(r+\rho)(r-\rho)^2}E\rho\,\mathrm{d}\rho = -p_z \tag{6a}$$

$$\begin{aligned}
&\beta C\frac{\partial\Delta u_z}{\partial r} + \frac{1}{\pi}\left(\frac{2\mu_1\mu_2}{\mu_1+\mu_2}-C\right)\int_{r_i}^{r_o}\Delta u_r\left\{\frac{r^2+\rho^2}{(r+\rho)(r-\rho)^2 r}E - \frac{1}{(r+\rho)r}K\right\}\mathrm{d}\rho\\
&\quad + \frac{2}{\pi}\left(C-\frac{\mu_1\mu_2}{\mu_1+\mu_2}\right)\int_{r_i}^{r_o}\Delta u_r\left[\left\{\frac{r^2+4r\rho+\rho^2}{(r+\rho)^3 r} + \frac{8r^2\rho^2}{(r+\rho)^3(r-\rho)^2 r}\right\}E - \frac{1}{(r+\rho)r}K\right]\mathrm{d}\rho = -p_x
\end{aligned} \tag{6b}$$

$$\left.\begin{aligned}
&\alpha = \frac{\mu_2(\kappa_1+1)-\mu_1(\kappa_2+1)}{\mu_2(\kappa_1+1)+\mu_1(\kappa_2+1)}, \quad \beta = \frac{\mu_2(\kappa_1-1)-\mu_1(\kappa_2-1)}{\mu_2(\kappa_1+1)+\mu_1(\kappa_2+1)}\\
&C = \frac{2\mu_1(1+\alpha)}{(1-\beta^2)(\kappa_1+1)} = \frac{2\mu_2(1-\alpha)}{(1-\beta^2)(\kappa_2+1)}
\end{aligned}\right\} \tag{6c}$$

Here, by substituting $r = r_c + r'$, $\rho = r_c + \rho'$ into Eqs. (6a), (6b) and putting $r_c \to \infty$, we obtain the following equations:

$$-\beta C\frac{\partial\Delta u_r}{\partial r} + \frac{C}{\pi}\int_{r_i}^{r_o}\Delta u_z\frac{1}{(r'-\rho')^2}\,\mathrm{d}\rho' = -p_z \tag{7a}$$

$$\beta C\frac{\partial \Delta u_z}{\partial r}+\frac{C}{\pi}\int_{r_i}^{r_o}\Delta u_r\frac{1}{(r'-\rho')^2}\,\mathrm{d}\rho' = -p_x \tag{7b}$$

These equations coincide with the equations of a two-dimensional interface crack subjected to uniform tension in z-direction (for example, Comninou, 1977).

3. Numerical solutions of singular integral equations

3.1. Torsion of a ring-shaped interface crack

Consider a ring-shaped interface crack under torsion at infinity as shown in Fig. 2. In the numerical solution of Eq. (3a), the unknown crack opening displacement Δu_θ is approximated by the product of the fundamental density function $w_\theta(\rho)$ and the weight function $F_{\mathrm{III}}(\rho)$:

$$\Delta u_\theta = \sum_{m=1}^{2}\left\{\frac{1}{\mu_m}w_\theta(\rho)\right\}F_{\mathrm{III}}(\rho) \tag{8}$$

Here, the fundamental density function is chosen exactly to express the stress field due to a single interface crack under anti-plane shear. The fundamental density function is given by (Rice and Sih, 1965)

$$\sum_{m=1}^{2}\frac{1}{\mu_m}w_\theta(\rho) = \sum_{m=1}^{2}\frac{1}{\mu_m}\frac{1+\kappa_m}{4}\sqrt{c^2-\rho^2} \tag{9}$$

In this numerical solution, the weight function $F_{\mathrm{III}}(\rho)$ is approximated by the following power series:

$$F_{\mathrm{III}}(\rho) = \sum_{n=1}^{M}a_n\rho^{n-1} \tag{10}$$

A set of collocation points is given by (Noda and Oda, 1997)

$$r = -c\cos\{n\pi/(M+1)\}+r_c \quad (n = 1,\ldots,M) \tag{11}$$

By using the numerical solution mentioned above, we finally obtain Eq. (12) by substituting Eqs. (8)–(10) into Eq. (3a):

$$\left.\begin{aligned}&\frac{1}{\pi}\sum_{n=1}^{M}a_nA_n = -p_y\\ &A_n = \int_{r_i}^{r_o}\sqrt{c^2-\rho^2}\left\{\frac{r^2+\rho^2}{(r+\rho)(r-\rho)^2r}E-\frac{1}{(r+\rho)r}K\right\}\rho^{n-1}\,\mathrm{d}\rho\end{aligned}\right\} \tag{12}$$

It should be noted that Eq. (12) does not include elastic constants of the materials. It is known that stress intensity factors of a two-dimensional interface crack under anti-plane shear are independent of elastic constants (Willis, 1971; Tucker, 1974; Erdogan and Gupta, 1975; Zhang, 1984; Delale, 1985). In a similar way, Eq. (12) shows that stress intensity factors of a ring-shaped interface crack under uniform torsion are also independent of elastic constants.

Since Eq. (12) has singularities when $r = \rho$, the following expansion forms are applied to evaluate the integrals. By substituting $\rho = r+\varepsilon$ into Eq. (12) and neglecting the higher terms than ε^2, we have

$$\int_{r-\varepsilon_0}^{r+\varepsilon_0} \sqrt{c^2-\rho^2}\left[\frac{r^2+\rho^2}{(r+\rho)(r-\rho)^2 r}E - \frac{1}{(r+\rho)r}K\right]F_{\mathrm{III}}(\rho)\,\mathrm{d}\rho$$
$$= \int_{-\varepsilon_0}^{\varepsilon_0} \sqrt{c^2-r^2}\frac{1}{\varepsilon^2}\left[1-\left(\frac{1}{c^2-r^2}-\frac{1}{2r}\right)\varepsilon - \left\{\frac{1}{2(c^2-r^2)}+\frac{c^2}{2(c^2-r^2)^2}-\frac{3}{16r^2}\right.\right.$$
$$\left.\left. + \frac{3}{8r^2}\ln\left(\frac{8r}{\varepsilon}\right)\right\}\varepsilon^2+\cdots\right]F_{\mathrm{III}}(\rho)\,\mathrm{d}\varepsilon \tag{13a}$$

where

$$\left.\begin{aligned} K(k) &= \ln(8r/\varepsilon) - \{\ln(8r/\varepsilon)-1\}\varepsilon^2/16r^2+\cdots \\ E(k) &= 1+\{\ln(8r/\varepsilon)-1/2\}\varepsilon^2/8r^2+\cdots \end{aligned}\right\} \tag{13b}$$

$$\left.\begin{aligned} F_{\mathrm{III}}(\rho) &= \textstyle\sum_{n=1}^{M} a_n\rho^{n-1} \\ \rho^{n-1} &= r^{n-1}+(n-1)r^{n-2}\varepsilon+\textstyle\sum_{j=0}^{n-3}\left\{(j+1)\rho^{(n-3-j)}r^j\right\}\varepsilon^2+\cdots \end{aligned}\right\} \tag{13c}$$

Using Eqs. (13) with suitably chosen ε_0, the integrals can be evaluated very accurately.

3.2. Tension of a ring-shaped interface crack

Consider a ring-shaped interface crack under tension at infinity. In the numerical solution of Eqs. (6a), (6b), the unknown crack opening displacements Δu_z, Δu_r are approximated by the product of the fundamental density function $w_z(\rho)$, $w_r(\rho)$ and the weight functions $F_1(\rho)$, $F_2(\rho)$:

$$\Delta u_z + \mathrm{i}\Delta u_r = \sum_{m=1}^{2}\left\{\frac{\kappa_m-1}{\mu_m(1+\kappa_m)}w_z(\rho)+\mathrm{i}\frac{1}{\mu_m}w_r(\rho)\right\}\{F_1(\rho)+\mathrm{i}F_2(\rho)\} \tag{14}$$

Here, the fundamental density functions are expressed by

$$\sum_{m=1}^{2}\left\{\frac{\kappa_m-1}{\mu_m(1+\kappa_m)}w_z(\rho)+\mathrm{i}\frac{1}{\mu_m}w_r(\rho)\right\} = \sum_{m=1}^{2}\frac{1}{\mu_m}\frac{1+\kappa_m}{4\cosh(\pi\gamma/\mathrm{i})}\sqrt{c^2-\rho^2}\left(\frac{c-\rho}{c+\rho}\right)^{\gamma} \tag{15}$$

Eqs. (14) and (15) express the exact solution for the two-dimensional interface crack subjected to internal pressure $\sigma_z = p$ or $\tau_{rz} = q$ (Rice and Sih, 1965; Nisitani et al., 1992, 1993). Here, γ is defined by

$$\gamma = \frac{1}{2\pi\mathrm{i}}\ln\left[(\mu_1\kappa_2+\mu_2)/(\mu_2\kappa_1+\mu_1)\right] \tag{16}$$

In this numerical solution, the weight functions $F_1(\rho)$, $F_2(\rho)$ are approximated by the following power series:

$$F_1(\rho) = \sum_{n=1}^{M} b_n\rho^{n-1}, \quad F_2(\rho) = \sum_{n=1}^{M} c_n\rho^{n-1} \tag{17}$$

We obtain the fundamental equations of a ring-shaped interface crack by substituting Eqs. (14)–(17) into Eqs. (6a), (6b):

$$\sum_{n=1}^{M}[b_nB_n + c_nC_n] = -p_z, \quad \sum_{n=1}^{M}[b_nD_n + c_nE_n] = -p_x \tag{18a}$$

$$\left.\begin{aligned}
B_n &= \frac{1}{4\cosh(\pi\gamma/\mathrm{i})}\left[-\frac{1-\mathrm{e}^{4\pi\gamma\mathrm{i}}}{\mathrm{e}^{2\pi\gamma\mathrm{i}}}\frac{\partial}{\partial r}\left\{\sqrt{c^2-r^2}g(r)r^{n-1}\right\}\right.\\
&\quad\left.+\frac{1}{\pi}\frac{1+\mathrm{e}^{4\pi\gamma\mathrm{i}}}{\mathrm{e}^{2\pi\gamma\mathrm{i}}}\int_{r_\mathrm{i}}^{r_\mathrm{o}}\sqrt{c^2-\rho^2}f(\rho)\frac{2}{(r+\rho)(r-\rho)^2}E\rho^n\,\mathrm{d}\rho\right]\\
C_n &= \frac{1}{4\cosh(\pi\gamma/\mathrm{i})}\left[\frac{1-\mathrm{e}^{4\pi\gamma\mathrm{i}}}{\mathrm{e}^{2\pi\gamma\mathrm{i}}}\frac{\partial}{\partial r}\left\{\sqrt{c^2-r^2}f(r)r^{n-1}\right\}\right.\\
&\quad\left.+\frac{1}{\pi}\frac{1+\mathrm{e}^{4\pi\gamma\mathrm{i}}}{\mathrm{e}^{2\pi\gamma\mathrm{i}}}\int_{r_\mathrm{i}}^{r_\mathrm{o}}\sqrt{c^2-\rho^2}g(\rho)\frac{2}{(r+\rho)(r-\rho)^2}E\rho^n\,\mathrm{d}\rho\right]\\
D_n &= \frac{1}{4\cosh(\pi\gamma/\mathrm{i})}\left[-\frac{1-\mathrm{e}^{4\pi\gamma\mathrm{i}}}{\mathrm{e}^{2\pi\gamma\mathrm{i}}}\frac{\partial}{\partial r}\left\{\sqrt{c^2-r^2}f(r)r^{n-1}\right\}\right.\\
&\quad\left.+\frac{1}{\pi}\frac{1+\mathrm{e}^{4\pi\gamma\mathrm{i}}}{\mathrm{e}^{2\pi\gamma\mathrm{i}}}\int_{r_\mathrm{i}}^{r_\mathrm{o}}\sqrt{c^2-\rho^2}g(\rho)\left\{\frac{r^2+\rho^2}{(r+\rho)(r-\rho)^2r}E+\frac{1}{(r+\rho)r}K\right\}\rho^{n-1}\,\mathrm{d}\rho\right]\\
E_n &= \frac{1}{4\cosh(\pi\gamma/\mathrm{i})}\left[\frac{1-\mathrm{e}^{4\pi\gamma\mathrm{i}}}{\mathrm{e}^{2\pi\gamma\mathrm{i}}}\frac{\partial}{\partial r}\left\{\sqrt{c^2-r^2}g(r)r^{n-1}\right\}\right.\\
&\quad\left.+\frac{1}{\pi}\frac{1+\mathrm{e}^{4\pi\gamma\mathrm{i}}}{\mathrm{e}^{2\pi\gamma\mathrm{i}}}\int_{r_\mathrm{i}}^{r_\mathrm{o}}\sqrt{c^2-\rho^2}f(\rho)\left\{\frac{r^2+\rho^2}{(r+\rho)(r-\rho)^2r}E+\frac{1}{(r+\rho)r}K\right\}\rho^{n-1}\,\mathrm{d}\rho\right]
\end{aligned}\right\}\tag{18b}$$

where

$$f(x)=\cos\left\{\ln\left(\frac{c+x}{c-x}\right)^{\gamma/\mathrm{i}}\right\},\quad g(x)=\sin\left\{\ln\left(\frac{c+x}{c-x}\right)^{\gamma/\mathrm{i}}\right\}$$

It should be noted that the stress intensity factors depend on γ only in a similar way of the ones of a penny-shaped interface crack (Kassir and Bregman, 1972) and a deep circumferential interface crack (Takakuda et al., 1978). A set of collocation points is given by Eq. (11). To evaluate the singular integrals in Eq. (18), we apply the following expansion forms in a similar way of Eq. (13):

$$\int_{r-\varepsilon_0}^{r+\varepsilon_0}\Delta u_z(\rho)\frac{2}{(r+\rho)(r-\rho)^2}E\rho\,\mathrm{d}\rho=\int_{-\varepsilon_0}^{\varepsilon_0}\Delta u_z(\rho)\frac{1}{\varepsilon^2}\left[1+\frac{\varepsilon}{2r}+\left\{-\frac{5}{16r^2}+\frac{1}{8r^2}\ln\left(\frac{8r}{\varepsilon}\right)\right\}\varepsilon^2+\cdots\right]\mathrm{d}\varepsilon\tag{19a}$$

$$\begin{aligned}
&\int_{r-\varepsilon_0}^{r+\varepsilon_0}\Delta u_r(\rho)\left\{\frac{r^2+\rho^2}{(r+\rho)(r-\rho)^2r}E-\frac{1}{(r+\rho)r}K\right\}\mathrm{d}\rho\\
&=\int_{r-\varepsilon_0}^{r+\varepsilon_0}\Delta u_r(\rho)\left[\left\{\frac{r^2+4r\rho+\rho^2}{(r+\rho)^3r}-\frac{8r^2\rho^2}{(r+\rho)^3(r-\rho)^2r}\right\}E-\frac{1}{(r+\rho)r}K\right]\mathrm{d}\rho\\
&=\int_{-\varepsilon_0}^{\varepsilon_0}\Delta u_r(\rho)\frac{1}{\varepsilon^2}\left[1+\frac{\varepsilon}{2r}+\left\{\frac{3}{16r^2}-\frac{3}{8r^2}\ln\left(\frac{8r}{\varepsilon}\right)\right\}\varepsilon^2+\cdots\right]\mathrm{d}\varepsilon
\end{aligned}\tag{19b}$$

$$\left.\begin{aligned}
&\Delta u_z(\rho)+\mathrm{i}\Delta u_r(\rho)=\textstyle\sum_{m=1}^{2}\dfrac{1}{\mu_m}\dfrac{1+\kappa_m}{4\cosh(\pi\gamma/\mathrm{i})}\sqrt{c^2-\rho^2}\left(\dfrac{c+\rho}{c-\rho}\right)^{\gamma}\{F_1(\rho)+\mathrm{i}F_2(\rho)\}\\
&\sqrt{c^2-\rho^2}\left(\dfrac{c+\rho}{c-\rho}\right)^{\gamma}=\sqrt{c^2-\rho^2}\left[\cos\left\{\ln\left(\dfrac{c+\rho}{c-\rho}\right)^{\gamma/\mathrm{i}}\right\}+\mathrm{i}\sin\left\{\ln\left(\dfrac{c+\rho}{c-\rho}\right)^{\gamma/\mathrm{i}}\right\}\right]\\
&\qquad=\sqrt{c^2-r^2}\left[\cos\left\{\ln\left(\dfrac{c+r}{c-r}\right)^{\gamma/\mathrm{i}}\right\}+\mathrm{i}\sin\left\{\ln\left(\dfrac{c+r}{c-r}\right)^{\gamma/\mathrm{i}}\right\}\right]\\
&\qquad\quad\times\left[1-\dfrac{\varepsilon}{c^2-r^2}(r-2c\gamma)-\dfrac{\varepsilon^2}{2(c^2-r^2)^2}\{(1-4\gamma^2)c^2-4cr\gamma\}+\cdots\right]\\
&F_1(\rho)+\mathrm{i}F_2(\rho)=\textstyle\sum_{n=1}^{M}b_n\rho^{n-1}+\mathrm{i}\sum_{n=1}^{M}c_n\rho^{n-1}\\
&\rho^{n-1}=r^{n-1}+(n-1)r^{n-2}\varepsilon+\textstyle\sum_{j=0}^{n-3}\left\{(j+1)\rho^{(n-3-j)}r^j\right\}\varepsilon^2+\cdots
\end{aligned}\right\}\quad(19\mathrm{c})$$

Using Eqs. (19) with suitably chosen ε_0, the integrals can be evaluated very accurately.

4. Numerical results and discussion

4.1. Convergence of the results

First, a ring-shaped interface crack under uniform tension $\sigma_z=\sigma$ is analyzed with varying the number of polynomials M in Eq. (17). Table 1 shows convergence of the results with increasing the collocation number M when $c/r_c=0.9$, $\gamma/\mathrm{i}=0.07$ and 0.15. Here, F_1^{i} denotes F_1 value at the inner tip $r=r_{\mathrm{i}}$ in Fig. 2, and F_1^{o} denotes F_1 value at the outer tip $r=r_{\mathrm{o}}$. In this analysis, generally, the convergence becomes slow as $c/r_c\to 1$ because of using two-dimensional solutions as the fundamental functions (see Eqs. (8) and (15)). However, Table 1 shows good convergence to the third digit at $M=13$ even when $c/r_c=0.9$.

Table 1
Convergence of the present result of interface crack when $c/r_c=0.9$. $K_1^{\mathrm{i}}-\mathrm{i}K_2^{\mathrm{i}}=(F_1^{\mathrm{i}}+\mathrm{i}F_2^{\mathrm{i}})\sigma\sqrt{\pi c}(1-2\gamma)$, $F_j^{\mathrm{i}}=F_j(r_{\mathrm{i}})$ $(j=1,2)$, $K_1^{\mathrm{i}}-\mathrm{i}K_2^{\mathrm{i}}=\lim_{r\to r_{\mathrm{i}}}\sqrt{2\pi(r_{\mathrm{i}}-r)}(\sigma_z-\mathrm{i}\tau_{rz})|_{z=0}\{(r_{\mathrm{i}}-r)/2c\}^{\gamma}$, $K_1^{\mathrm{o}}+\mathrm{i}K_2^{\mathrm{o}}=(F_1^{\mathrm{o}}+\mathrm{i}F_2^{\mathrm{o}})\sigma\sqrt{\pi c}(1+2\gamma)$, $F_j^{\mathrm{o}}=F_j(r_{\mathrm{o}})$ $(j=1,2)$, $K_1^{\mathrm{o}}+\mathrm{i}K_2^{\mathrm{o}}=\lim_{r\to r_{\mathrm{o}}}\sqrt{2\pi(r-r_{\mathrm{o}})}(\sigma_z+\mathrm{i}\tau_{rz})|_{z=0}\{(r-r_{\mathrm{o}})/2c\}^{\gamma}$

γ/i	M	F_1^{i}	F_2^{i}	F_1^{o}	F_2^{o}
0.07	6	2.143	0.105	0.883	0.026
	7	2.501	0.107	0.907	0.013
	8	2.559	0.107	0.892	0.022
	9	2.597	0.106	0.901	0.016
	10	2.621	0.104	0.896	0.020
	11	2.629	0.103	0.896	0.019
	12	2.650	0.102	0.898	0.020
	13	2.656	0.098	0.898	0.018
0.15	6	2.530	0.248	0.862	0.056
	7	2.633	0.255	0.878	0.027
	8	2.703	0.258	0.870	0.046
	9	2.750	0.256	0.874	0.032
	10	2.781	0.253	0.872	0.041
	11	2.794	0.249	0.871	0.037
	12	2.817	0.243	0.873	0.038
	13	2.827	0.238	0.873	0.036

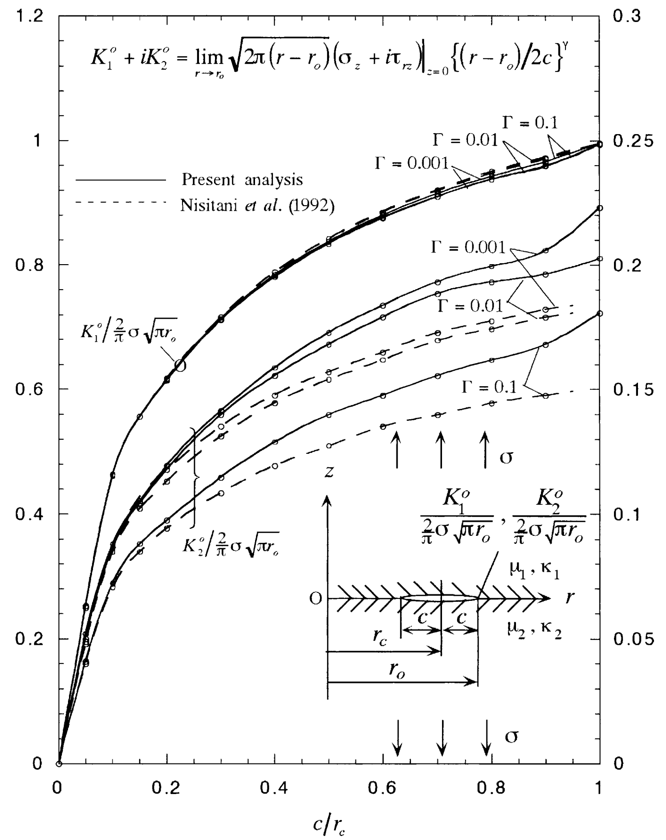

Fig. 3. $K_1^o/\frac{2}{\pi}\sigma\sqrt{\pi r_o}$ and $K_2^o/\frac{2}{\pi}\sigma\sqrt{\pi r_o}$ at the outer tip of ring-shaped interface crack ($\Gamma = M_2/M_1$: shear modulus ratio).

In Fig. 3, present results are compared with the results of Nisitani et al. (1992) with varying c/r_c and $\Gamma = \mu_2/\mu_1$ systematically, where the closed form solution of a penny-shaped interface crack is also indicated at $c/r_c \to 1$ (Kassir and Bregman, 1972). Regarding tension-type stress intensity factors at the outer tip $K_1^o/(2/\pi)\sigma\sqrt{\pi r_o}$, both present results and Nisitani's ones are in good agreement with the exact solution as $c/r_c \to 1$. However, regarding shear-type stress intensity factors $K_2^o/(2/\pi)\sigma\sqrt{\pi r_o}$ at the outer tip, the present results seem more reliable because they are in better agreement with the exact solution as $c/r_c \to 1$.

4.2. Results of a ring-shaped interface crack under torsion

In Table 2 and Fig. 4, stress intensity factors of a ring-shaped interface crack under torsion are shown with varying c/r_c. Here, $F_{\mathrm{III}}^{\mathrm{i}}$ denotes F_{III} value at the inner tip $r = r_{\mathrm{i}}$ in Fig. 2, and $F_{\mathrm{III}}^{\mathrm{o}}$ denotes F_{III} value at the outer tip $r = r_{\mathrm{o}}$. As shown in Fig. 4, the value of $F_{\mathrm{III}}^{\mathrm{o}}$ coincide with the results of a penny-shaped interface crack as $c/r_c \to 1$ under torsion (Erdogan, 1965).

4.3. Results of a ring-shaped interface crack under tension

In Tables 3, 4 and Figs. 5, 6, stress intensity factors of a ring-shaped interface crack under uniform tension are shown with varying γ/i and c/r_c systematically. In Table 3 the exact solution for a penny-shaped

Table 2
Dimensionless stress intensity factors $F^{\mathrm{i}}_{\mathrm{III}}$, $F^{\mathrm{o}}_{\mathrm{III}}$ of interface crack. $F^{\mathrm{i}}_{\mathrm{III}} = K^{\mathrm{i}}_{\mathrm{III}}/(r_{\mathrm{i}}/r_{\mathrm{o}})\tau\sqrt{\pi c}$, $K^{\mathrm{i}}_{\mathrm{III}} = \lim_{r\to r_{\mathrm{i}}}\sqrt{2\pi(r_{\mathrm{i}}-r)}\tau_{z\theta}|_{z=0}$, $F^{\mathrm{o}}_{\mathrm{III}} = K^{\mathrm{o}}_{\mathrm{III}}/\tau\sqrt{\pi c}$, $K^{\mathrm{o}}_{\mathrm{III}} = \lim_{r\to r_{\mathrm{o}}}\sqrt{2\pi(r-r_{\mathrm{o}})}\tau_{z\theta}|_{z=0}$, $F^{\mathrm{i}}_{\mathrm{III}} = F_{\mathrm{III}}(r_{\mathrm{i}})$, $F^{\mathrm{o}}_{\mathrm{III}} = F_{\mathrm{III}}(r_{\mathrm{o}})$

c/r_c	$F^{\mathrm{i}}_{\mathrm{III}}$	$F^{\mathrm{o}}_{\mathrm{III}}$
$\to 0.0$	1.000	1.000
0.1	1.018	0.970
0.2	1.027	0.935
0.3	1.027	0.899
0.4	1.019	0.864
0.5	1.002	0.831
0.6	0.973	0.801
0.7	0.928	0.773
0.8	0.857	0.748
0.9	0.724	0.726
$\to 1.0$		0.707

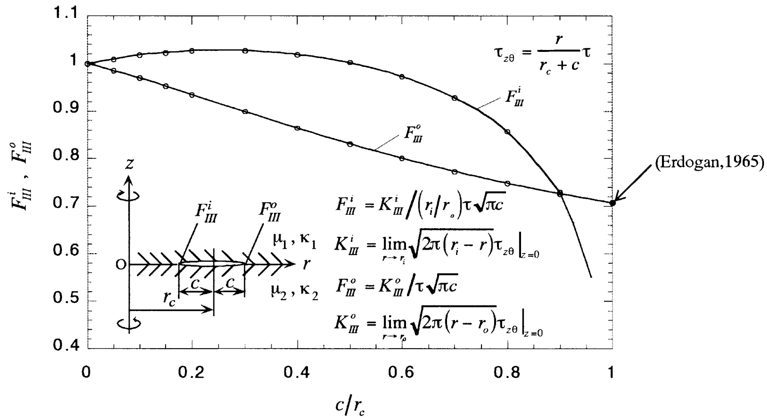

Fig. 4. $F^{\mathrm{i}}_{\mathrm{III}}$ and $F^{\mathrm{o}}_{\mathrm{III}}$ at the inner tip and outer tip of ring-shaped interface crack.

interface crack is indicated at $c/r_c \to 1$. The stress intensity factor is given in a closed form as shown in Eq. (20) (Kassir and Bregman, 1972):

$$K^{\mathrm{o}}_1 + \mathrm{i}K^{\mathrm{o}}_2 \to \frac{2}{\pi}\sigma\sqrt{\pi c} \times F(\gamma)(c/r_c \to 1), \quad F(\gamma) = \sqrt{\pi}\frac{\Gamma(2+\gamma)}{\Gamma\left(\frac{1}{2}+\gamma\right)}, \quad \Gamma(z) = \int_0^\infty \mathrm{e}^{-t}t^{z-1}\,\mathrm{d}t \tag{20}$$

In Tables 3 and 4, the results for $\gamma/\mathrm{i} = 0$–0.15 are shown, whose values are corresponding to most cases of material combinations (Sih and Chen, 1981). As shown in Figs. 5 and 6, the present results coincide with the results of two-dimensional interface crack as $c/r_c \to 0$. Next, in Fig. 7, normalized values of $K^{\mathrm{o}}_1/(2/\pi)\sigma\sqrt{\pi r_{\mathrm{o}}}$ and $K^{\mathrm{o}}_2/(2/\pi)\sigma\sqrt{\pi r_{\mathrm{o}}}$ are shown to be compared with the exact solution for a penny-shaped interface crack. As shown in Fig. 7, the present results at the outer tip coincide with the exact solution as $c/r_c \to 1$.

On the other hand, in Fig. 8, normalized results at the inner tip $K^{\mathrm{i}}_1/(1/2)\sigma_{\mathrm{net}}\sqrt{\pi r_{\mathrm{i}}}$ and $K^{\mathrm{i}}_2/(1/2)\sigma_{\mathrm{net}}\sqrt{\pi r_{\mathrm{i}}}$ are shown. Here, σ_{net} is the nominal stress defined by Eq. (21) (Table 5):

$$\sigma_{\mathrm{net}} = \frac{1}{\pi r_{\mathrm{i}}^2}\int_0^{r_{\mathrm{i}}} 2\pi r\sigma_z\Big|_{z=0}\mathrm{d}r \tag{21}$$

Table 3
Dimensionless stress intensity factors $K_1^o/\sigma\sqrt{\pi c}$, $K_2^o/\sigma\sqrt{\pi c}$ of ring-shaped interface crack. $K_1^o + iK_2^o = \lim_{r\to r_o}\sqrt{2\pi(r-r_o)}(\sigma_z + i\tau_{rz})|_{z=0}\{(r-r_o)/2c\}^{\gamma}$

	c/r_c	γ/i															
		0.00	0.01	0.02	0.03	0.04	0.05	0.06	0.07	0.08	0.09	0.10	0.11	0.12	0.13	0.14	0.15
$\frac{K_1^o}{\sigma\sqrt{\pi c}}$	$\to$ 0.0	1.000	1.000	1.000	1.000	1.000	1.000	1.000	1.000	1.000	1.000	1.000	1.000	1.000	1.000	1.000	1.000
	0.1	0.979	0.979	0.979	0.979	0.978	0.978	0.978	0.977	0.977	0.976	0.976	0.975	0.975	0.974	0.973	0.972
	0.2	0.963	0.962	0.962	0.962	0.962	0.961	0.961	0.960	0.959	0.958	0.957	0.956	0.955	0.953	0.952	0.950
	0.3	0.950	0.949	0.949	0.949	0.948	0.948	0.946	0.946	0.945	0.943	0.942	0.940	0.938	0.936	0.934	0.932
	0.4	0.939	0.939	0.938	0.938	0.937	0.936	0.935	0.934	0.933	0.931	0.929	0.927	0.925	0.922	0.919	0.916
	0.5	0.930	0.930	0.929	0.929	0.928	0.927	0.926	0.924	0.922	0.920	0.918	0.916	0.913	0.910	0.906	0.903
	0.6	0.922	0.922	0.922	0.921	0.920	0.919	0.917	0.916	0.914	0.911	0.909	0.906	0.903	0.899	0.895	0.891
	0.7	0.916	0.915	0.915	0.914	0.913	0.912	0.910	0.908	0.906	0.903	0.900	0.897	0.894	0.890	0.885	0.881
	0.8	0.910	0.910	0.909	0.908	0.907	0.906	0.904	0.902	0.899	0.896	0.893	0.889	0.885	0.881	0.876	0.871
	0.9	0.903	0.903	0.903	0.903	0.902	0.900	0.897	0.895	0.892	0.891	0.886	0.882	0.879	0.871	0.866	0.862
	$\to 1.0^{(15)}$	0.900	0.900	0.900	0.900	0.899	0.899	0.898	0.897	0.896	0.895	0.894	0.893	0.891	0.890	0.888	0.886
$\frac{K_2^o}{\sigma\sqrt{\pi c}}$	$\to$0.0	0.0000	0.0200	0.0400	0.0600	0.0800	0.1000	0.1200	0.1400	0.1600	0.1800	0.2000	0.2200	0.2400	0.2600	0.2800	0.3000
	0.1	0.0000	0.0200	0.0401	0.0601	0.0801	0.1001	0.1202	0.1402	0.1601	0.1802	0.2002	0.2202	0.2401	0.2601	0.2800	0.3000
	0.2	0.0000	0.0201	0.0402	0.0604	0.0805	0.1006	0.1207	0.1407	0.1608	0.1808	0.2009	0.2209	0.2409	0.2608	0.2807	0.3005
	0.3	0.0000	0.0202	0.0404	0.0606	0.0808	0.1010	0.1210	0.1413	0.1614	0.1815	0.2015	0.2218	0.2415	0.2614	0.2813	0.3010
	0.4	0.0000	0.0203	0.0406	0.0610	0.0812	0.1014	0.1218	0.1419	0.1623	0.1822	0.2023	0.2224	0.2422	0.2620	0.2819	0.3015
	0.5	0.0000	0.0204	0.0408	0.0612	0.0816	0.1019	0.1221	0.1424	0.1627	0.1828	0.2029	0.2228	0.2427	0.2625	0.2821	0.3017
	0.6	0.0000	0.0205	0.0410	0.0614	0.0819	0.1023	0.1226	0.1429	0.1631	0.1833	0.2034	0.2231	0.2430	0.2627	0.2821	0.3014
	0.7	0.0000	0.0206	0.0411	0.0617	0.0822	0.1026	0.1230	0.1433	0.1635	0.1837	0.2036	0.2235	0.2435	0.2625	0.2817	0.3008
	0.8	0.0000	0.0207	0.0413	0.0619	0.0824	0.1029	0.1234	0.1439	0.1641	0.1842	0.2042	0.2240	0.2436	0.2629	0.2822	0.3010
	0.9	0.0000	0.0206	0.0417	0.0620	0.0827	0.1041	0.1249	0.1457	0.1664	0.1851	0.2052	0.2234	0.2436	0.2618	0.2803	0.2999
	$\to 1.0^{(15)}$	0.0000	0.0215	0.0430	0.0645	0.0859	0.1074	0.1289	0.1504	0.1719	0.1934	0.2150	0.2365	0.2580	0.2795	0.3011	0.3226

Table 4
Dimensionless stress intensity factors $K_1^{\mathrm{i}}/\sigma\sqrt{\pi c}$, $-K_2^{\mathrm{i}}/\sigma\sqrt{\pi c}$ of ring-shaped interface crack. $K_1^{\mathrm{i}} - \mathrm{i}K_2^{\mathrm{i}} = \lim_{r\to r_{\mathrm{i}}} \sqrt{2\pi(r_{\mathrm{i}} - r)}(\sigma_z - \mathrm{i}\tau_{rz})|_{z=0}\{(r_{\mathrm{i}} - r)/2c\}^{\gamma}$

	c/r_c	γ/i															
		0.00	0.01	0.02	0.03	0.04	0.05	0.06	0.07	0.08	0.09	0.10	0.11	0.12	0.13	0.14	0.15
$\frac{K_1^{\mathrm{o}}}{\sigma\sqrt{\pi c}}\to$	0.0	1.000	1.000	1.000	1.000	1.000	1.000	1.000	1.000	1.000	1.000	1.000	1.000	1.000	1.000	1.000	1.000
	0.1	1.030	1.030	1.030	1.030	1.030	1.030	1.031	1.031	1.032	1.032	1.033	1.034	1.035	1.036	1.037	1.038
	0.2	1.068	1.068	1.068	1.069	1.069	1.070	1.071	1.072	1.073	1.074	1.075	1.077	1.079	1.081	1.083	1.085
	0.3	1.118	1.118	1.118	1.119	1.120	1.121	1.122	1.123	1.125	1.127	1.130	1.132	1.135	1.139	1.142	1.146
	0.4	1.182	1.182	1.183	1.184	1.185	1.187	1.188	1.191	1.194	1.197	1.200	1.204	1.208	1.213	1.218	1.224
	0.5	1.269	1.269	1.270	1.271	1.273	1.275	1.278	1.281	1.285	1.289	1.294	1.299	1.305	1.312	1.319	1.327
	0.6	1.390	1.390	1.391	1.393	1.395	1.398	1.402	1.407	1.412	1.418	1.425	1.432	1.440	1.450	1.460	1.470
	0.7	1.572	1.573	1.574	1.577	1.580	1.584	1.590	1.596	1.603	1.612	1.621	1.632	1.643	1.656	1.670	1.685
	0.8	1.884	1.885	1.887	1.891	1.896	1.903	1.910	1.920	1.931	1.943	1.957	1.973	1.992	2.009	2.030	2.052
	0.9	2.576	2.577	2.580	2.587	2.595	2.606	2.620	2.636	2.655	2.677	2.698	2.728	2.757	2.788	2.820	2.854
$\frac{K_2^{\mathrm{j}}}{\sigma\sqrt{\pi c}}\to$	0.0	0.0000	0.0200	0.0400	0.0600	0.0800	0.1000	0.1200	0.1400	0.1600	0.1800	0.2000	0.2200	0.2400	0.2600	0.2800	0.3000
	0.1	0.0000	0.0200	0.0400	0.0600	0.0801	0.1001	0.1201	0.1401	0.1601	0.1801	0.2002	0.2203	0.2403	0.2604	0.2806	0.3007
	0.2	0.0000	0.0202	0.0404	0.0605	0.0807	0.1009	0.1211	0.1413	0.1615	0.1818	0.2020	0.2223	0.2426	0.2629	0.2832	0.3036
	0.3	0.0000	0.0205	0.0409	0.0614	0.0818	0.1023	0.1228	0.1433	0.1639	0.1844	0.2050	0.2256	0.2463	0.2669	0.2877	0.3084
	0.4	0.0000	0.0209	0.0418	0.0628	0.0837	0.1047	0.1256	0.1466	0.1677	0.1887	0.2099	0.2310	0.2522	0.2735	0.2948	0.3162
	0.5	0.0000	0.0217	0.0433	0.0650	0.0867	0.1084	0.1302	0.1520	0.1738	0.1957	0.2177	0.2397	0.2618	0.2839	0.3062	0.3285
	0.6	0.0000	0.0228	0.0457	0.0685	0.0915	0.1145	0.1375	0.1605	0.1836	0.2069	0.2302	0.2536	0.2771	0.3007	0.3244	0.3480
	0.7	0.0000	0.0248	0.0497	0.0746	0.0996	0.1245	0.1496	0.1748	0.2001	0.2255	0.2511	0.2768	0.3028	0.3288	0.3550	0.3830
	0.8	0.0000	0.0285	0.0571	0.0857	0.1144	0.1432	0.1722	0.2014	0.2305	0.2600	0.2895	0.3191	0.3499	0.3810	0.4111	0.4420
	0.9	0.0000	0.0370	0.0742	0.1114	0.1488	0.1863	0.2242	0.2624	0.3003	0.3401	0.3798	0.4187	0.4590	0.5009	0.5420	0.5821

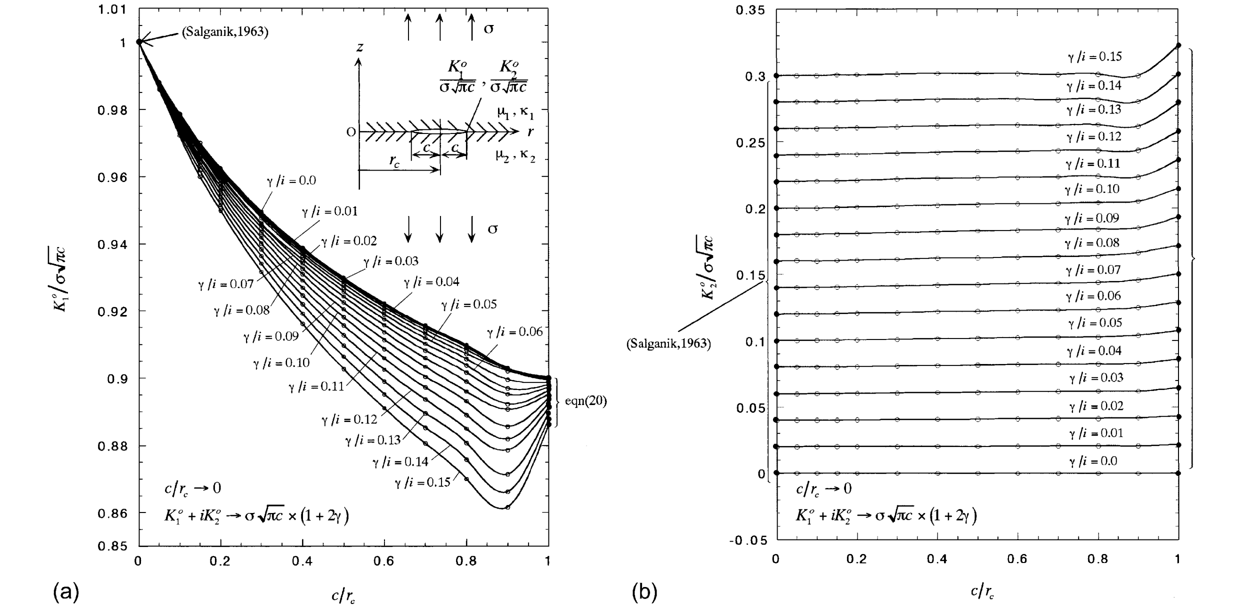

Fig. 5. Stress intensity factors at the outer tip of ring-shaped interface crack ($K_1^o + iK_2^o = \lim_{r \to r_o} \sqrt{2\pi(r - r_o)}(\sigma_z + i\tau_{rz})|_{z=0}\{(r - r_o)/2c\}^{\gamma}$): (a) $K_1^o/\sigma\sqrt{\pi c}$, (b) $K_2^o/\sigma\sqrt{\pi c}$.

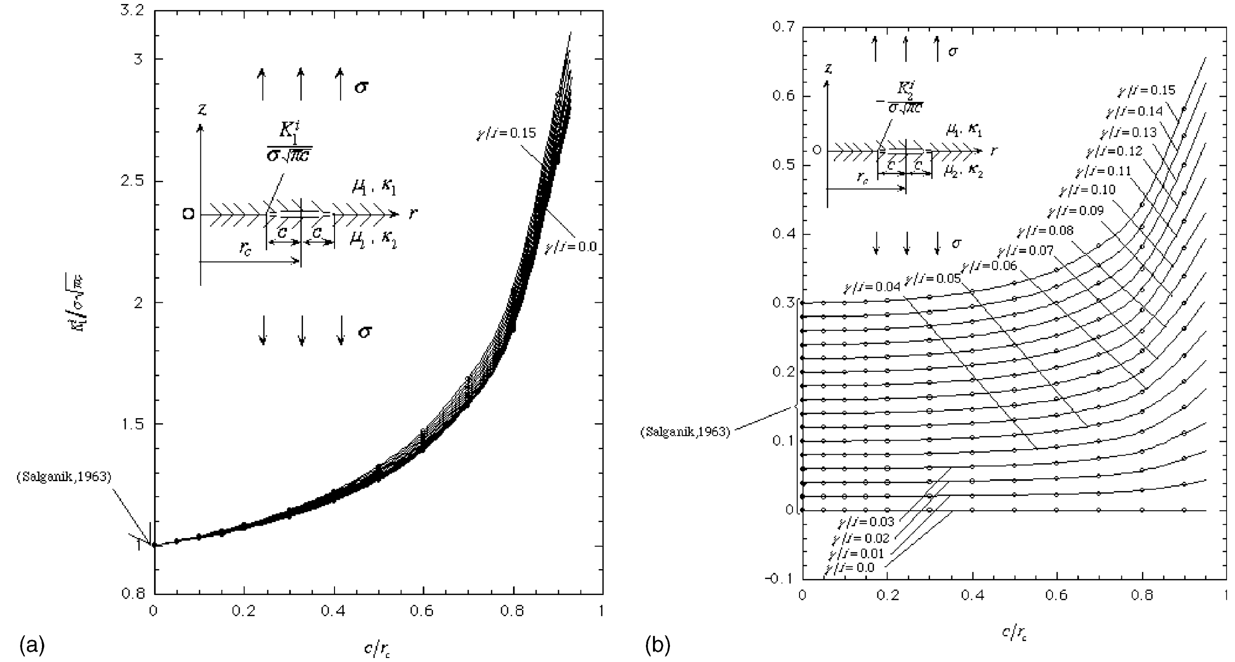

Fig. 6. Stress intensity factors at the inner tip of ring-shaped interface crack ($K_1^i - iK_2^i = \lim_{r \to r_i} \sqrt{2\pi(r_i - r)}(\sigma_z - i\tau_{rz})|_{z=0}\{(r_i - r)/2c\}^{\gamma}$): (a) $K_1^i/\sigma\sqrt{\pi c}$, (b) $-K_2^i/\sigma\sqrt{\pi c}$.

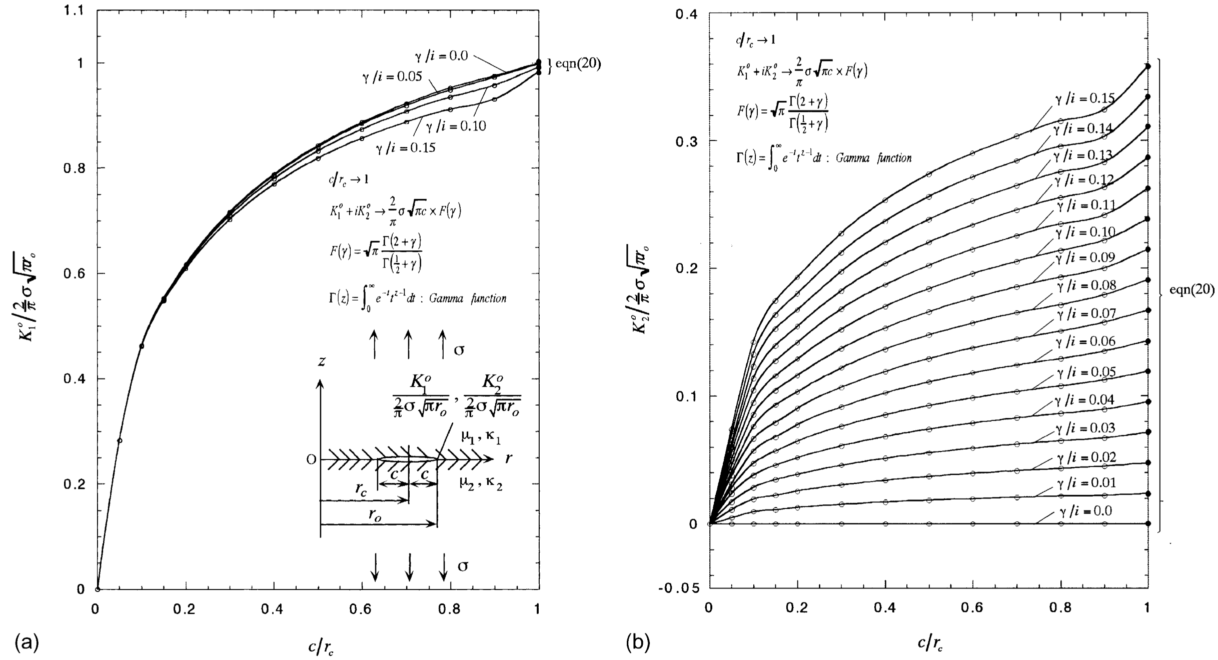

Fig. 7. Stress intensity factors at the outer tip of ring-shaped interface crack ($K_1^o + iK_2^o = \lim_{r\to r_o} \sqrt{2\pi(r - r_o)}(\sigma_z + i\tau_{rz})|_{z=0}\{(r - r_o)/2c\}^{\gamma}$): (a) $K_1^o/\frac{2}{\pi}\sigma\sqrt{\pi r_o}$, (b) $K_2^o/\frac{2}{\pi}\sigma\sqrt{\pi r_o}$.

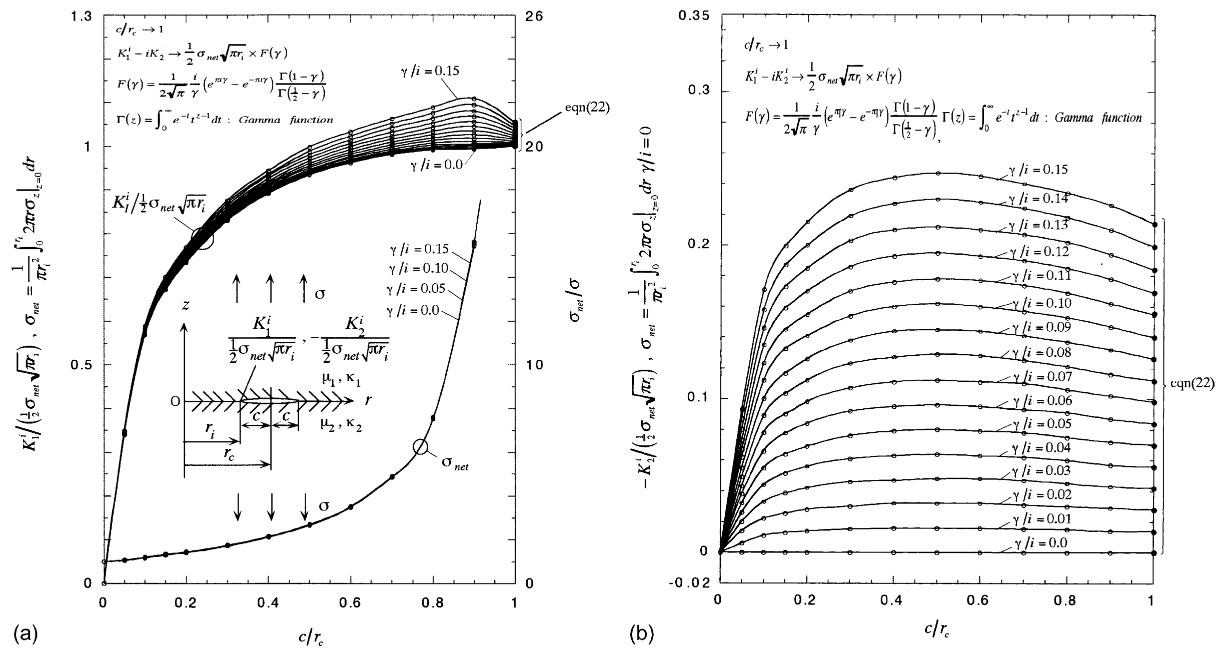

Fig. 8. Stress intensity factors at the inner tip of ring-shaped interface crack ($K_1^i - iK_2^i = \lim_{r\to r_i} \sqrt{2\pi(r_i - r)}(\sigma_z - i\tau_{rz})|_{z=0}\{(r_i - r)/2c\}^{\gamma}$): (a) $K_1^i/(\frac{1}{2}\sigma_{net}\sqrt{\pi r_i})$, (b) $-K_2^i/(\frac{1}{2}\sigma_{net}\sqrt{\pi r_i})$.

Table 5
$\sigma_{\text{net}}/\sigma$ at the inside of ring-shaped interface crack. $\sigma_{\text{net}} = \frac{1}{\pi r_i^2}\int_0^{r_i} 2\pi r \sigma_z|_{z=0}\,\mathrm{d}r$

c/r_c	γ/i			
	0.00	0.05	0.10	0.15
→ 0.0	1.000	1.000	1.000	1.000
0.1	1.209	1.207	1.197	1.176
0.2	1.456	1.453	1.437	1.411
0.3	1.763	1.758	1.742	1.714
0.4	2.163	2.159	2.141	2.116
0.5	2.716	2.712	2.694	2.660
0.6	3.537	3.534	3.517	3.485
0.7	4.898	4.893	4.876	4.842
0.8	7.606	7.594	7.570	7.534
0.9	15.65	15.58	15.50	15.44

The stress intensity factors for a deep circumferential interface crack are given by Eq. (22) as a closed form (Takakuda et al., 1978):

$$\begin{aligned} &K_1^{\mathrm{i}} - \mathrm{i}K_2^{\mathrm{i}} \to \frac{1}{2}\sigma_{\text{net}}\sqrt{\pi r_{\mathrm{i}}} \times F(\gamma)(c/r_c \to 1) \\ &F(\gamma) = \frac{1}{2\sqrt{\pi}}\frac{\mathrm{i}}{\gamma}(\mathrm{e}^{\pi\mathrm{i}\gamma} - \mathrm{e}^{-\pi\mathrm{i}\gamma})\frac{\Gamma(1-\gamma)}{\Gamma\left(\frac{1}{2}-\gamma\right)}, \quad \Gamma(z) = \int_0^\infty \mathrm{e}^{-t}t^{z-1}\,\mathrm{d}t \end{aligned} \tag{22}$$

As shown in Fig. 8, the present results, K_1^{i} and K_2^{i}, coincide with the exact solution as $c/r_c \to 1$.

5. Conclusions

In this paper, three-dimensional interface cracks were considered by using the singular integral equations of the body force method. The stress intensity factors of a ring-shaped interface crack subjected to torsion or tension at infinity were calculated systematically. The conclusion can be made as follows:

(1) In the numerical solution, the unknown functions were approximated by the fundamental density functions and power series. It was found that the method gives rapidly converging numerical results (see Table 1) under various geometrical conditions and material combinations (see Tables 3 and 4).
(2) For a ring-shaped interface crack under torsion, the results were independent of the elastic constants similarly to the case of two-dimensional interface cracks subjected to anti-plane shear. The stress intensity factors were shown in table and chart when the value of c/r_c were changed systematically (see Table 2 and Fig. 4).
(3) For a ring-shaped interface crack under tension, the results depended on γ only as shown in Eq. (18). The stress intensity factors were shown in charts with varying γ/i and c/r_c systematically (see Figs. 5–8).
(4) The present results coincided with the solutions of a two-dimensional interface crack as $c/r_c \to 0$. On the other hand, as $c/r_c \to 1$, the present results at the outer tip coincided with the exact solution for a penny-shaped interface crack given by Kassir and Bregman (see Fig. 7(a), (b)). Also as $c/r_c \to 1$, the present results at the inner tip coincided with the solution for a deep circumferential interface crack given by Takakuda et al., 1978 (see Fig. 8(a), (b)).

References

Chen, M.-C., Noda, N.-A., Tang, R., 1999. Application of finite-part integrals to planar interfacial fracture problems in three-dimensional bimaterials. ASME J. Appl. Mech. 66, 885–890.

Comninou, M., 1977. The interface crack. J. Appl. Mech. 44, 631–636.

Delale, F., 1985. Mode-III fracture of bonded nonhomogeneous materials. Engng. Fract. Mech. 22, 213–226.

England, A.H., 1965. A crack between dissimilar media. J. Appl. Mech. 32, 400–402.

Erdogan, F., 1963. Stresses distribution in a nonhomogeneous elastic plane with crack. J. Appl. Mech. 30, 232–236.

Erdogan, F., 1965. Stress distribution in bonded dissimilar materials containing circular or ring-shaped cavities. Trans. ASME Ser. E: J. Appl. Mech. 32, 829–836.

Erdogan, F., Gupta, G.D., 1975. Bonded wedges with an interface crack under anti-plane shear loading. Int. J. Fract. 11, 583–593.

Kassir, M.K., Bregman, A.M., 1972. The stress intensity factor for a penny-shaped crack between two dissimilar materials. Trans. ASME Ser. E: J. Appl. Mech. 39, 308–310.

Keer, L.M., Chen, S.H., Comninou, M., 1978. The interface penny-shaped crack reconsidered. Int. J. Engng. Sci. 16, 765–772.

Lowengrub, M., Sneddon, I.N., 1974. The effect of internal pressure on a penny-shaped crack at the interface of two bonded dissimilar elastic half-spaces. Int. J. Engng. Sci. 12, 387–396.

Mossakovski, V.I., Rybka, M.T., 1964. Generalization of the Griffith–Sneddon criterion for the case of a nonhomogeneous body. Prikl. Mat. Mekh. 28, 1061–1069.

Nisitani, H., Saimoto, A., Noguchi, H., 1993. Analysis of an interface crack based on the body force method. Trans. Jpn. Soc. Mech. Engrs. 59, 68–73 (in Japanese).

Nisitani, H., Saimoto, A., Noguchi, H., Chen, D.-H., 1992. Analysis of a symmetrical interface crack based on body force method. In: Proceedings of the 1992 Annual Meeting of JSME/MMD, 920, 72, pp. 237–238 (in Japanese).

Noda, N.-A., Oda, K., 1997. Interaction effect of stress intensity factors for any number of collinear interface cracks. Int. J. Fract. 84, 117–128.

Rice, J.R., Sih, G.C., 1965. Plane problem of cracks in dissimilar media. J. Appl. Mech. 32, 418–423.

Salganik, R.L., 1963. The brittle fracture of cemented bodies. Prikl. Mat. Mekh. 27, 957–962.

Sibuya, T., Koizumi, T., Iwamoto, T., 1989. Stress analysis of the vicinity of an elliptical crack at the interface of two bonded half-spaces. JSME Int. J. 32, 485–491.

Sih, G.C., Chen, E.P., 1981. Cracks in Composite Materials. In: Sih, G.C. (Ed.), Mechanics of Fracture, vol. VI. Martinus Nijhoff Publishers, Hague (Chapter 3).

Takakuda, K., Sibuya, T., Koizumi, T., 1978. Stress analysis for bimaterial with an interface crack. In: Prelim. Proc. 55th Annual Meeting of Japan Soc. Mech. Engrs., 780, 3, pp. 167–169 (in Japanese).

Tucker, M.O., 1974. Cracks in two-phase solids under longitudinal shear loading. Int. J. Fract. 10, 323–336.

Willis, J.R., 1971. Fracture mechanics of interfacial crack. J. Mech. Phys. Solids 19, 353–368.

Willis, J.R., 1972. The penny-shaped crack on an interface. Q. J. Mech. Appl. Math. 25, 367–385.

Yuuki, R., Cho, S.-B., 1989. Boundary element analysis of stress intensity factors for an interface crack in dissimilar materials. Trans. Jpn. Soc. Mech. Engrs. 55, 340–347 (in Japanese).

Zhang, X.S., 1984. A central crack at the interface between two different media in a rectangular sheet under anti-plane shear. Engng. Fract. Mech. 19, 709–715.